

## THE GEODETIC MONITORING OF THE ENGINEERING STRUCTURE – A PRACTICAL SOLUTION OF THE PROBLEM IN 3D SPACE

Daria Filipiak-Kowszyk <sup>1</sup>, Artur Janowski <sup>1,2</sup>, Waldemar Kamiński <sup>1,2</sup>,  
Karolina Makowska <sup>1</sup>, Jakub Szulwic <sup>1</sup>, Krzysztof Wilde <sup>1</sup>

<sup>1</sup>) Faculty of Civil and Environmental Engineering, Gdansk University of Technology,  
Gdansk, Poland

<sup>2</sup>) Faculty of Geodesy, Geospatial and Civil Engineering,  
University of Warmia and Mazury, Olsztyn, Poland

### Abstract

*The study raises the issues concerning the automatic system designed for the monitoring of movement of controlled points, located on the roof covering of the Forest Opera in Sopot. It presents the calculation algorithm proposed by authors. It takes into account the specific design and location of the test object. High forest stand makes it difficult to use distant reference points. Hence the reference points used to study the stability of the measuring position are located on the ground elements of the six-meter-deep concrete foundations, from which the steel arches are derived to support the roof covering (membrane) of the Forest Opera. The tacheometer used in the measurements is located in the glass body placed on a special platform attached to the steel arcs. Measurements of horizontal directions, vertical angles and distances can be additionally subject to errors caused by the laser beam penetration through the glass. Dynamic changes of weather conditions, including the temperature and pressure also have a significant impact on the value of measurement errors, and thus the accuracy of the final determinations represented by the relevant covariance matrices. The estimated coordinates of the reference points, controlled points and tacheometer along with the corresponding covariance matrices obtained from the calculations in the various epochs are used to determine the significance of acquired movements. In case of the stability of reference points, the algorithm assumes the ability to study changes in the position of tacheometer in time, on the basis of measurements performed on these points.*

**Keywords:** displacement, monitoring, adjustment

## 1. Introduction

The monitoring system of the Forest Opera was created after the modernization of the object roofing. The main contractor of the monitoring system is Wilde Engineering company from Gdansk. The authors of this paper presented the analysis of the accuracy of the obtained movements values. The observations subjected to the analysis were taken from the online system which continuously processes data and presents them in closed Internet system. The design and installation of the system were described in the article (Wilde et al., 2015). After starting the monitoring system and commissioning of the new roof covering of the Forest Opera, the series of control measures was performed on the basis of the terrestrial laser scanning – TLS (Janowski et al., 2015) and subsequently developed using the FEM finite elements method. Additionally, the performed measurements confirmed the correct location of the box with the measuring instrument (total station with phase rangefinder) and its structure made of glass walls, placed obliquely in order to minimize the impact of the Snellius law on the diffraction of the beams of laser passing through the 3-millimeter glass which acts as a plane-parallel plate. For the monitoring results the change of the laser beam angle may be significant only in case of significant movement values of controlled points (for the analyzed object it can be assumed that these values are even 1 m), with which we have to deal in case of the deformation of the technical fabric which is the component of the roof covering (Fig. 1).

The largest displacement of up to 1.2 m, was observed at a distance of 50 m from the tachometer, which is reflected by the change in the measurement of the vertical angle by 1.4 degree (1.5 grade). Controlled points located closer were characterized by lower values of displacements, which was in turn reflected by the change of angular values by no more than 0.5 degrees. The construction of the total station box (Fig. 3) is designed so that the laser beam can fall orthogonally onto a glass partition (no effect on the angular measurement) with a maximum deviation of 20 degrees. Experimental studies conducted in the Team of Department of Geodesy of Gdansk University of Technology and analysis of the results (Daliga, 2014, Daliga and Kuralowicz, 2016) indicate that the change in the angle of laser beam incidence on the glass partition of the total station box is reflected by the error of point location at the level not higher than 0.08 mm and it applies to only one controlled point on the roof covering. Therefore, this value can be neglected in the analysis.

Box with measuring station (total station) was located on a platform above the audience, at the level of controlled points. This solution had an impact on the stability of the measuring station (which was analyzed in an article), however it made it possible to reduce the effect of refraction when passing through the air layers of a various density.

When designing the project, which was the installation of a monitoring system, there were fears that the instability of the tachometer and reference points will prevent the effective determination of displacements of the roof covering structure in the Forest Opera. Therefore, the authors performed the analysis of the single- and two-stage adjustment of the geodetic network (tachometer, controlled points and the reference points). The assumed accuracy of determining the displacement was measured at centimetres level.

## 2. Monitoring system of the Forest Opera in Sopot

First information concerning Forest Opera dates back to the early twentieth and the roofing of the object was made in 1964. Due to the fact that it was leaking and there was a need for its disassembly during winter season, it was decided to rebuild the facility. The current, modern design (Fig. 1.) was commissioned in 2012 and thanks to its appearance it is integrated into the forest nature of the place. The design assumed that the leaf-shaped roof covering will be made of a technical fabric with the thickness less than 1 mm, and a maximum span of the roof is 104 m and a length of 85 m.

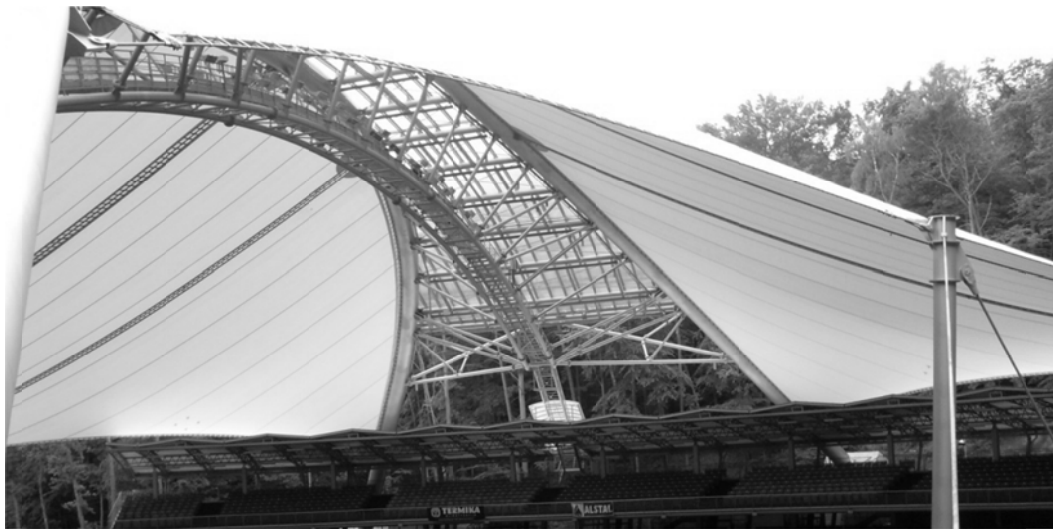


**Fig. 1.** View onto the structure of Forest Opera

Due to the relatively custom design, which was selected at the design phase of the Forest Opera, it was required to discover a modern method of checking parameters related to the construction work and safety. Taking into account the characteristics of the facility, the most important seem to be the monitoring of the movements of a roof covering. It is very important, because the covering will not be disassembled during the winter season and the displacement related to the accumulation of snow can be significant, which in turn may even lead to the rupture of the membrane. The good solution to the above problem is the automatic monitoring system, which construction is shown schematically in the Fig. 2.

The main component of the measuring module is Leica TS 15I tacheometer (total station) along with the prisms representing the controlled points on the technical fabric, in total: 28. The system is made in such a way as to enable the determination of the current coordinates of the controlled points.

One of the problems encountered during the design phase of the system was the lack of a stable and at the same time a safe place, which could be used as station for the tacheometer. Due to this fact, it was decided to place the instrument on the special platform attached to the monitored structure, which causes that the total station can change its position in time. Tacheometer location is shown in the Fig. 3.

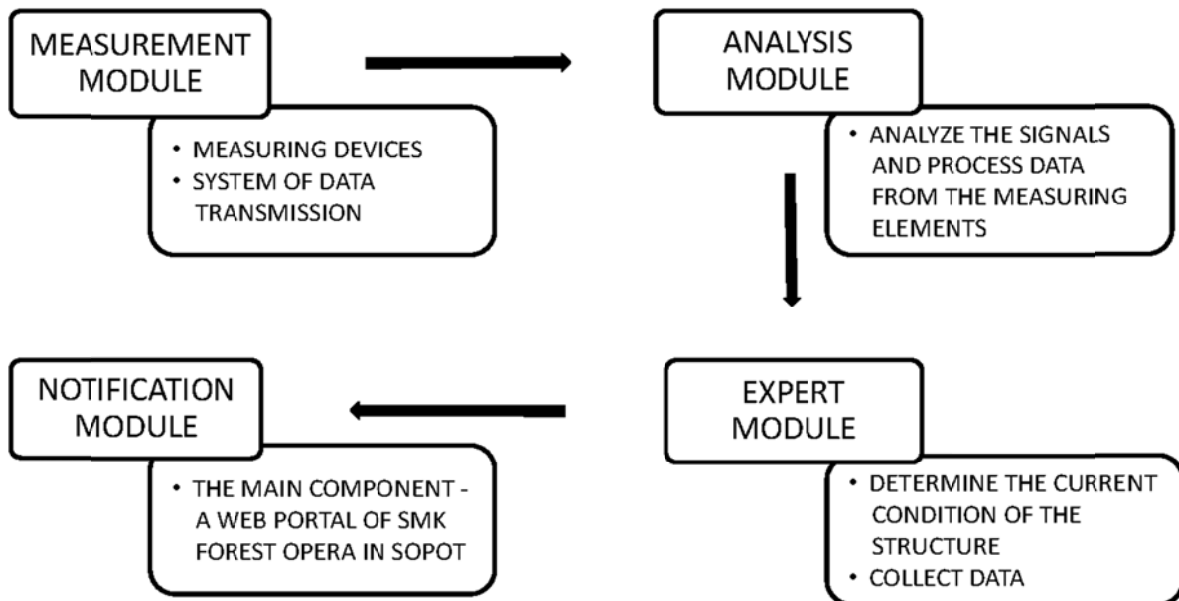


**Fig. 2.** Scheme of the Forest Opera monitoring system

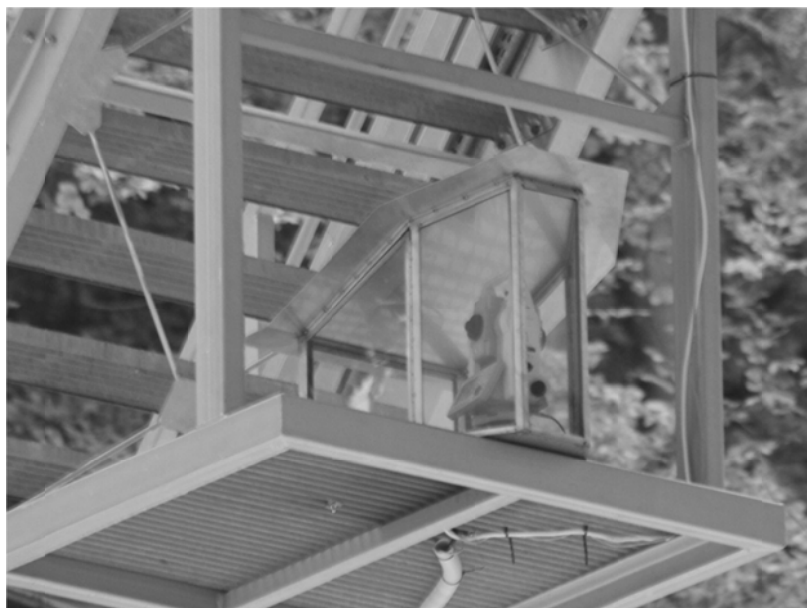


**Fig. 3.** Location of the measuring station (total station)

The article proposes a post-processing algorithm of data processing which uses the measurements performed for the reference and controlled points. Reference points were mounted on three foundations on which the main arcs supporting the covering structure are based. Assuming the stability of their position, which should be confirmed, it is possible to determine the tacheometer movement. Sketch of the network is shown in Fig. 4., where the numbers of 29, 30 and 31 are reference points, the letter T indicates the total station and  $\alpha_i$  ( $i = 29, 30, 31$ ) is a vertical angle.

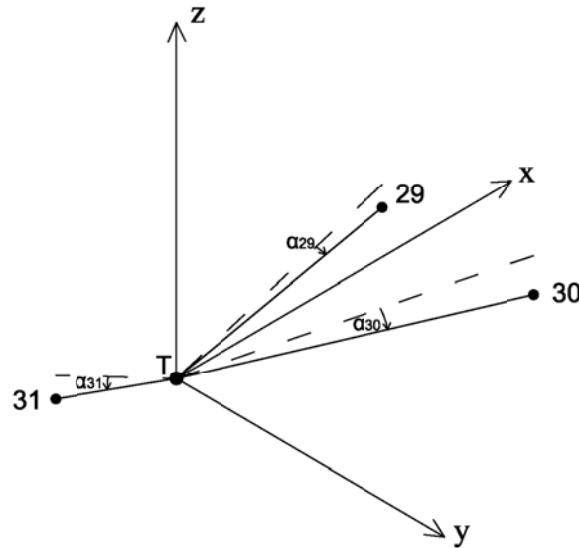


Fig. 4. Reference points network

### 3. Study of the stability of reference points and displacements of controlled points

#### 3.1. Theoretical basis of the free adjustment

Study of points displacement can be carried out in single or two stage process. One-stage approach involves the simultaneous investigation of the stability of reference points with the determination of controlled points displacements. Using a two-stage approach while, at first we study the stability of reference points, and then we determine the displacement of the controlled points.

One way of determining the displacements and detecting the unstable reference points is the IWST method - Iterative Weighted Similarity Transformation - (Chen, 1983; Chen et al., 1990). It involves an iterative transformation of differences in adjusted coordinates using a weighting function. IWST method belongs to the group of robust methods.

In this paper, checking the stability of reference points has been carried out using only the results of free adjustment (Perelmuter, 1979; Wisniewski, 2013). The following shows only the most important assumptions of this method of estimation, because they are required to understand the presented method for identifying the points stability.

In the free estimation we do not accept a priori the stability of any point. In the performed analyses, for the purpose of the determination of points stability authors used the ellipses of confidence (for horizontal position) and mean errors of height for the vertical position.

The task of free adjustment (Perelmuter, 1979; Wisniewski, 2013) can be represented in the following form:

$$\left. \begin{aligned} \hat{\mathbf{v}} &= \mathbf{A}\hat{\mathbf{d}}_x + \mathbf{L} \\ \varphi(\mathbf{d}_x) &= \hat{\mathbf{v}}^T \mathbf{P}\hat{\mathbf{v}} = \min \\ \varphi_x(\mathbf{d}_x) &= \hat{\mathbf{d}}_x^T \mathbf{P}_x \hat{\mathbf{d}}_x = \min \end{aligned} \right\} \quad (1)$$

where:

$\mathbf{A}$  - matrix of known coefficients  $\mathbf{A} = [\mathbf{A}_1 \quad \vdots \quad \mathbf{A}_2]$ , where the number of columns in the  $\mathbf{A}_2$  submatrix is equal to the established defect of the geodetic network,

$\mathbf{P}$  - matrix of weights,

$\mathbf{P}_x$  - matrix of weights of the points coordinates (obtained e.g. from the previous determinations,  $\mathbf{P}_x = \hat{\mathbf{C}}_x^{-1}$ ,  $\hat{\mathbf{C}}_x$  - estimated covariance matrix),

$\mathbf{L}$  - vector of free terms (observation results),

$\hat{\mathbf{v}}$  - the estimated vector of corrections,

$\hat{\mathbf{d}}_x$  - the estimated vector of unknowns.

From the above-cited works, it results that the problem (1) may be led to the following compensatory task:

$$\left. \begin{aligned} \mathbf{B}\hat{\mathbf{d}}_x + \mathbf{A}_1^T \mathbf{P}\mathbf{L} &= \mathbf{0} \\ \varphi_x(\mathbf{d}_x) = \hat{\mathbf{d}}_x^T \mathbf{P}_x \hat{\mathbf{d}}_x &= \min \end{aligned} \right\} \quad (2)$$

where:

$$\mathbf{B} = [\mathbf{A}_1^T \mathbf{P} \mathbf{A}_1 \quad \vdots \quad \mathbf{A}_1^T \mathbf{P} \mathbf{A}_2].$$

When looking for the solution of the task (2) we will obtain:

$$\hat{\mathbf{d}}_x = -\mathbf{P}_x^{-1} \mathbf{B}^T (\mathbf{B} \mathbf{P}_x^{-1} \mathbf{B}^T)^{-1} \mathbf{A}_1^T \mathbf{P} \mathbf{L} = -\mathbf{A}^+ \mathbf{L} \quad (3)$$

where:

$\mathbf{A}^+ = -\mathbf{P}_x^{-1} \mathbf{B}^T (\mathbf{B} \mathbf{P}_x^{-1} \mathbf{B}^T)^{-1} \mathbf{A}_1^T \mathbf{P}$  is the generalized inverse of the minimum norm in the least squares method. The problem of the generalized inverse of matrix was mentioned also in (Bjerhammer, 1951; Penrose, 1955). In the further adjustment process, the matrix of  $\mathbf{P}_x = \mathbf{I}$  was assumed ( $\mathbf{I}$  – identity matrix).

After determining the estimator of corrections  $\hat{\mathbf{v}} = \mathbf{A} \hat{\mathbf{d}}_x + \mathbf{L}$ , we are able to calculate the estimator of the variance coefficient  $\hat{\sigma}_0^2 = m_0^2$

$$m_0^2 = \frac{\hat{\mathbf{v}}^T \mathbf{P} \hat{\mathbf{v}}}{n - r + d} \quad (4)$$

where:

$n$  – number of observations,  $r$  – number of parameters,  $d$  – defect of the geodetic network.

### 3.2. Analysis of the accuracy and the study of points stability

In order to identify the stability of reference points it is necessary to determine  $\hat{\mathbf{C}}_x$  covariance matrix of adjusted coordinates for each measurement epoch:

$$\hat{\mathbf{C}}_x^{(j)} = m_0^2 \mathbf{P}_x^{-1} \mathbf{B}^T (\mathbf{B} \mathbf{P}_x^{-1} \mathbf{B}^T)^{-1} \mathbf{A}_1^T \mathbf{P} \mathbf{A}_1 (\mathbf{B} \mathbf{P}_x^{-1} \mathbf{B}^T)^{-1} \mathbf{B} \mathbf{P}_x^{-1} \quad j=(A,P) \quad (5)$$

As it is known the horizontal displacement of  $d_i$  can be determined from the following relation:

$$d_i = \sqrt{\Delta\hat{X}_i^2 + \Delta\hat{Y}_i^2} \quad (6)$$

in which:

$$\begin{aligned} \Delta\hat{X}_i &= \hat{X}_i^A - \hat{X}_i^P \\ \Delta\hat{Y}_i &= \hat{Y}_i^A - \hat{Y}_i^P \end{aligned} \quad (7)$$

and A - the designation of the actual measurement, P – the designation of the initial measurement.

On the basis of  $\hat{C}_{\hat{x}} = \hat{C}_{\hat{x}}^{(P)} + \hat{C}_{\hat{x}}^{(A)}$  covariance matrix, it was possible to determine the confidence ellipse for the displacement of each point (Caspary, 2000).

Displacements of points in the vertical plane are analyzed on the basis of the difference of  $\Delta\hat{Z}_i = \hat{Z}_i^A - \hat{Z}_i^P$  and the value of the mean error for  $m_{\Delta\hat{Z}_i}$  displacement.

**One-step approach:** Determination of displacement of the controlled point no. 1, located on the membrane, while the study of the reference points.

Table 1 shows the results of the adjustment, obtained from the calculations performed in accordance with the previously described dependencies. The values of weights were computed based on the measurements mean errors for vertical angle  $m_\alpha = 5^{cc}$ , horizontal angle  $m_\beta = 5^{cc}$  and distance  $m_l = 0.5 \text{ mm}$ .

**Table 1.** Results obtained from the free adjustment for the initial and actual measurement

No.	Point Coordinate	Initial measurement (P)		Actual measurement (A)		Displacements $\Delta\hat{X}, \Delta\hat{Y}, \Delta\hat{Z}$ [mm]
		Increment $\hat{d}_x$ [mm]	Adjusted coordinates [mm]	Increment $\hat{d}_x$ [mm]	Adjusted coordinates [mm]	
T	$\hat{X}$	2.9	1.5	-0.1	-1.5	-3.0
	$\hat{Y}$	0.4	0.6	0.8	1.0	0.4
	$\hat{Z}$	-0.1	-3.1	2.5	-0.5	2.6
29	$\hat{X}$	1.5	79689.3	0.9	79688.7	-0.6
	$\hat{Y}$	0.4	-18519.4	0.0	-18519.8	-0.4
	$\hat{Z}$	-0.9	-5890.7	-1.5	-5891.3	-0.6
30	$\hat{X}$	1.0	84288.3	1.0	84288.3	0.0
	$\hat{Y}$	2.3	22217.8	-1.1	22214.4	-3.4
	$\hat{Z}$	-3.3	-9972.6	-3.1	-9972.4	0.2
31	$\hat{X}$	-1.8	-17279.1	-4.3	-17281.6	-2.5
	$\hat{Y}$	-1.3	-18815.6	-1.9	-18816.2	-0.6
	$\hat{Z}$	4.0	-5997.2	3.6	-5997.6	-0.4
1	$\hat{X}$	-3.7	18661.4	2.6	18667.7	6.3
	$\hat{Y}$	-1.9	-48384.9	2.2	-48380.8	4.1
	$\hat{Z}$	0.3	-2686.3	-1.5	-2688.1	-1.8

Based on the above data, the vectors for the  $d$  horizontal displacement for individual points were calculated. Results are presented in Table 2.

**Table 2.** Vectors  $d$  of horizontal displacements and their components of  $\Delta\hat{X}$ ,  $\Delta\hat{Y}$

Point no.	$\Delta\hat{X}$ [mm]	$\Delta\hat{Y}$ [mm]	$d$ [mm]
T	-3.0	0.4	3.0
29	-0.6	-0.4	0.7
30	0.0	-3.4	3.4
31	-2.5	-0.6	2.6
1	6.3	4.1	7.5

In order to verify the significance of the determined horizontal displacements, the confidence ellipses were determined (Fig. 5.). The value of  $F_{\gamma=0,95}$  was assumed in the calculations.

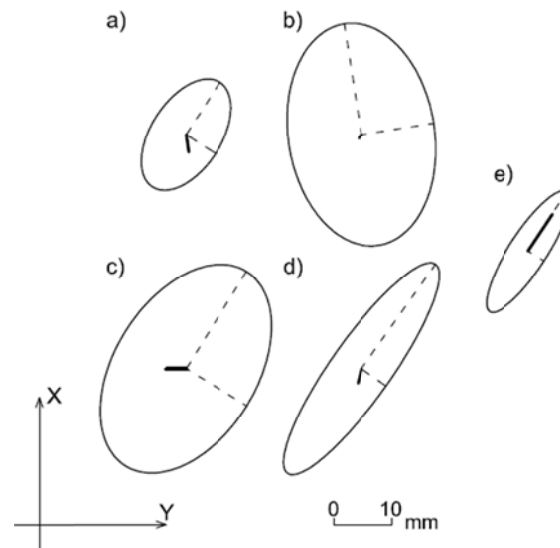


**Fig. 5.** Confidence ellipses for: a) tacheometer, b) 29 point, c) 30 point, d) 31 point, e) 1 point

The geometry of the network and measurement mean errors had an impact on obtained confidence ellipses. Horizontal displacements determined for individual points are included in confidence ellipses determined for them, which means that the designated displacements are not significant. Also the displacements in the vertical plane were subjected to analysis.

Table 3 below presents the values of the obtained displacements  $\Delta\hat{Z}$  and the corresponding values of mean errors of  $m_{\Delta\hat{Z}_i}$  for the chosen points. If  $|\Delta\hat{Z}| \leq km_{\Delta\hat{Z}_i}$ , then the displacement is considered as insignificant. The coefficient of  $k = 1$  was assumed for the purpose of the calculations.

**Table 3.** Significance of the displacements in the vertical plane

Point no.	$\Delta\hat{Z}$ [mm]	$m_{\Delta\hat{z}_i}$ [mm]	Displacement significance
T	2.6	2.2	<b>Significant</b>
29	-0.6	5.3	Insignificant
30	0.2	5.6	Insignificant
31	-0.4	2.7	Insignificant
1	-1.8	2.8	Insignificant

The analyzes conducted for horizontal and vertical plane returned results that clearly indicate that the points 29, 30 and 31 can be considered stable and not displaced, however they indicate the vertical displacement of the tacheometer.

**Two-stage approach:** Examination of the stability of reference points and the tacheometer (first stage), and then – the determination of the displacements of the controlled point no.1, located on the membrane (second stage).

For the purpose of analyses, the same observation results were used as in case of the single-stage approach. Table 4 presents the adjustment results, obtained from calculations. The values of weights were computed based on the measurements mean errors for vertical angle  $m_\alpha = 5^{cc}$ , horizontal angle  $m_\beta = 5^{cc}$  and distance  $m_l = 0.5 \text{ mm}$ .

**Table 4.** Results obtained from the free adjustment for the initial and actual measurement

No.	Point Coordinate	Initial measurement (P)		Actual measurement (A)		Displacements $\Delta\hat{X}, \Delta\hat{Y}, \Delta\hat{Z}$ [mm]
		Increment $\hat{d}_x$ [mm]	Adjusted coordinates [mm]	Increment $\hat{d}_x$ [mm]	Adjusted coordinates [mm]	
T	$\hat{X}$	1.6	0.2	0.0	-1.4	-1.6
	$\hat{Y}$	-0.4	-0.2	0.1	0.3	0.5
	$\hat{Z}$	-1.6	-4.6	0.4	-2.6	2.0
29	$\hat{X}$	0.1	79687.9	1.3	79689.1	1.2
	$\hat{Y}$	-0.8	-18520.6	0.6	-18519.2	1.4
	$\hat{Z}$	-2.3	-5892.1	-3.6	-5893.4	-1.3
30	$\hat{X}$	-0.4	84286.9	-0.1	84287.2	0.3
	$\hat{Y}$	0.9	22216.4	-0.7	22214.8	-1.6
	$\hat{Z}$	0.3	-9969.0	0.3	-9969.0	0.0
31	$\hat{X}$	-1.3	-17278.6	-1.3	-17278.6	0.0
	$\hat{Y}$	0.2	-18814.1	-0.1	-18814.4	-0.3
	$\hat{Z}$	3.6	-5997.6	3.0	-5998.2	-0.6

Similar to the single-stage approach, the vectors of displacement  $d$  were determined for the individual points. Results are presented in Table 5.

**Table 5.** Vectors  $d$  of horizontal displacements and their components of  $\Delta\hat{X}$ ,  $\Delta\hat{Y}$

Point no.	$\Delta\hat{X}$ [mm]	$\Delta\hat{Y}$ [mm]	$d$ [mm]
T	-1.6	0.5	1.7
29	1.2	1.4	1.8
30	0.3	-1.6	1.6
31	0.0	-0.3	0.3

For the examination of points stability, the confidence ellipses were used (Fig. 6). Similar to the single-stage approach, for the purpose of calculations the value of  $F_{\gamma=0,95}$  was assumed.

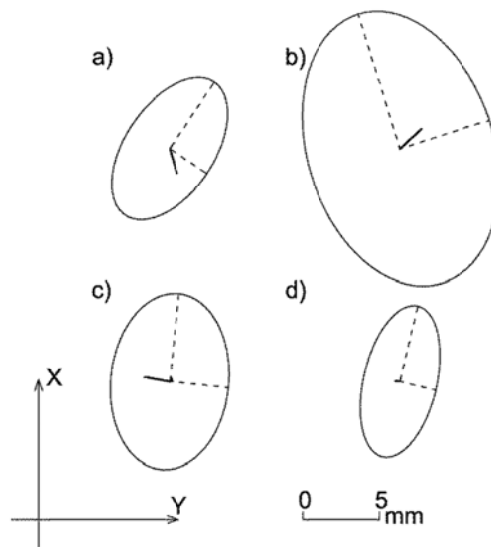


**Fig. 6.** Confidence ellipses for: a) tacheometer, b) 29 point, c) 30 point, d) 31 point

The above analyses indicate that the horizontal displacements determined for the individual points are included in the confidence ellipses determined for them. Also the displacements in the vertical plane were subjected to analysis. Table 6 presents the obtained results and values of mean errors of  $m_{\Delta\hat{Z}_i}$ .

**Table 6.** Significance of the displacements in the vertical plane

Point no.	$\Delta\hat{Z}$ [mm]	$m_{\Delta\hat{Z}_i}$ [mm]	Displacement significance
T	2.0	1.5	<b>Significant</b>
29	-1.3	3.0	Insignificant
30	0.0	0.2	Insignificant
31	-0.6	1.7	Insignificant

It results from the above analyses that 29, 30 and 31 points can be considered as stable and not displaced, however they indicate the tacheometer displacement.

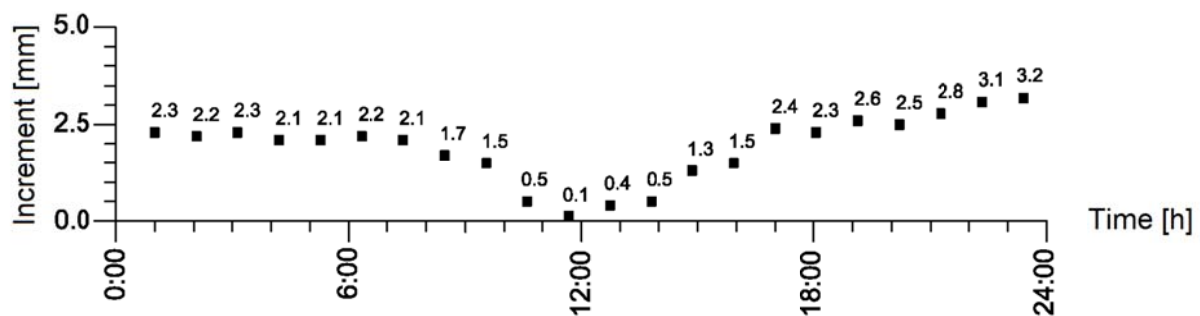
The obtained results constitute the basis for the determination of tacheometer station movement, on the basis of the observations carried out to the reference points (horizontal direction, vertical angle, distance).

Table 7 shows the results of adjustment carried out for the data throughout the day and night, whereas symbols of  $\hat{d}_{\Delta X}$ ,  $\hat{d}_{\Delta Y}$  and  $\hat{d}_{\Delta Z}$  mean the corresponding components of tacheometer movement and  $m_{\hat{d}_{\Delta X}}$ ,  $m_{\hat{d}_{\Delta Y}}$ ,  $m_{\hat{d}_{\Delta Z}}$  are corresponding values of mean errors (bold font indicates the significance of the increment).

**Table 7.** Increments for the initial coordinates of the tacheometer and their mean errors

Hour (epoch)	$\hat{d}_{\Delta X}$ [mm]	$m_{\hat{d}_{\Delta X}}$ [mm]	$\hat{d}_{\Delta Y}$ [mm]	$m_{\hat{d}_{\Delta Y}}$ [mm]	$\hat{d}_{\Delta Z}$ [mm]	$m_{\hat{d}_{\Delta Z}}$ [mm]
1:00 (1)	<b>2.3</b>	2.0	-1.1	1.7	<b>-2.8</b>	1.5
2:04 (2)	<b>2.2</b>	1.9	-1.0	1.7	<b>-3.0</b>	1.4
3:08 (3)	<b>2.3</b>	2.0	-0.9	1.7	<b>-3.2</b>	1.4
4:12 (4)	<b>2.1</b>	2.0	-0.9	1.7	<b>-3.2</b>	1.4
5:16 (5)	<b>2.1</b>	2.0	-1.1	1.7	<b>-3.3</b>	1.4
6:20 (6)	<b>2.2</b>	2.1	-1.3	1.8	<b>-3.5</b>	1.5
7:24 (7)	<b>2.1</b>	2.1	-1.1	1.8	<b>-3.2</b>	1.5
8:28 (8)	<b>1.7</b>	2.0	-1.4	1.7	<b>-2.9</b>	1.4
9:32 (9)	1.5	1.8	-1.0	1.5	<b>-2.6</b>	1.3
10:36 (10)	0.5	1.9	-0.3	1.6	<b>-1.9</b>	1.4
11:40 (11)	0.1	1.6	-1.1	1.4	-0.2	1.2
12:44 (12)	0.4	2.2	-0.2	1.9	<b>2.0</b>	1.6
13:48 (13)	0.5	1.6	-0.1	1.4	<b>1.7</b>	1.2
14:52 (14)	1.3	2.1	0.2	1.8	1.2	1.5
15:56 (15)	1.5	1.5	-0.8	1.3	0.3	1.1
17:00 (16)	<b>2.4</b>	1.7	-0.6	1.5	-0.2	1.2
18:04 (17)	<b>2.3</b>	1.7	-1.2	1.5	-1.1	1.2
19:08 (18)	<b>2.6</b>	1.7	-1.2	1.5	<b>-1.4</b>	1.2
20:12 (19)	<b>2.5</b>	1.7	-1.2	1.5	<b>-2.1</b>	1.2
21:16 (20)	<b>2.8</b>	1.9	-1.1	1.6	<b>-2.4</b>	1.3
22:20 (21)	<b>3.1</b>	1.9	-1.3	1.7	<b>-2.6</b>	1.4
23:24 (22)	<b>3.2</b>	1.9	-1.4	1.6	<b>-2.9</b>	1.4

These analyzes show the insignificance of the tachymeter movement with respect to the coordinate Y. Since this fact, the authors decided to present graphically the results of calculations – tacheometer movement, only for the X and Z coordinates (Fig. 7, Fig. 8).



**Fig. 7.** Increments for the X coordinate of the tacheometer

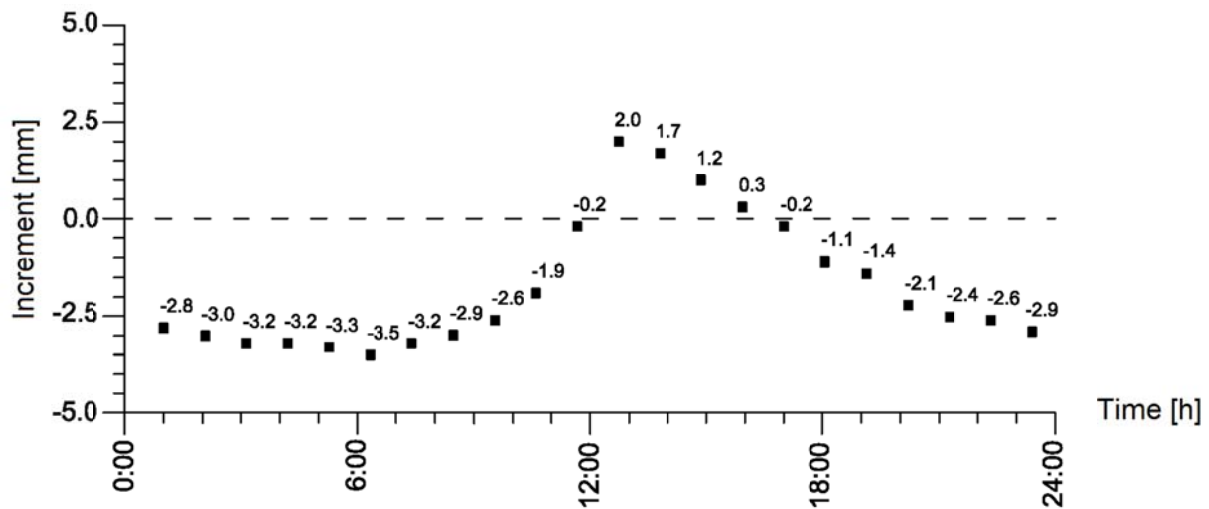


**Fig. 8.** Increments for the Z coordinate of the tacheometer

Analyses (Table 7, Fig. 7, Fig. 8) indicate that a change in the position of tacheometer station within the examined period of time is not significant. However, it exists and it is associated with the expansion of the structure that results from its warming during noon-hours.

At the second stage of the calculation of the described algorithm, the analyzes the displacement of controlled point no. 1 were performed. Using the adjusted coordinates of the tacheometer (from the 11<sup>th</sup> epoch) the adjustment is carried out and it results in adjusted coordinates of the point no. 1. The examination is carried out for two epochs, similar to those selected in a one-stage procedure. Table 8. presents the adjustment results, obtained from calculations.

**Table 8.** Results obtained from the adjustment for the initial and actual measurement

No.	Point Coordinate	Initial measurement ( <i>P</i> )		Actual measurement ( <i>A</i> )		Displacements $\Delta\hat{X}$ , $\Delta\hat{Y}$ , $\Delta\hat{Z}$ [mm]
		Increment $\hat{d}_x$ [mm]	Adjusted coordinates [mm]	Increment $\hat{d}_x$ [mm]	Adjusted coordinates [mm]	
1	$\hat{X}$	-11.5	18653.6	7.6	18672.7	19.1
	$\hat{Y}$	-5.8	-48388.8	1.0	-48382.0	6.8
	$\hat{Z}$	-3.2	-2689.8	-9.0	-2695.6	-5.9

#### 4. Summary

From the performer practical tests it results that the measurements of the examined facility are carried out with the accuracy, required for such structure.

Comparing the two approaches it can be seen that for the analyzed data (identical for both approaches) it was obtained significant differences between the displacements of the controlled point no. 1 - up to 13 mm for the X coordinate. This value results mainly from the fact that the one-stage approach does not assume a priori the stability of the any point position, so for each point the increments are calculated to the coordinates, and in a two-stage approach increments will be determined only for the position of tacheometer and point no. 1. Obtained coordinate differences (Table 1 and 8) can be caused by the adoption of stability of points no.

29, 30 and 31 in the two-stage approach. This was not assumed in one-step approach. Therefore in two-stage approach the coordinates of point no. 1 were computed based on earlier determined stable points. Both methods allow to select the displacement points. Moreover they let us to obtain the acceptable accuracy of results for analyzed structure.

On the background of different constantly monitored engineering structures described in the literature (eg. Bond et al., 2007; Berberan et al., 2007; Chrzanowski and Wilkins, 2006; Kohut et al., 2014; Pingue, 2011; Kowalczyk and Rapinski, 2014) the Forest Opera is one of the objects, characterized by the sub-meter displacements of controlled points and the obtained accuracy of their measurement at centimetres level exceeds the needs of the covering monitoring. So it can be concluded that the tachometer movement (drift) has a negligible impact on the interpretation of the obtained results of displacement in the situation of the lack of additional construction load.

### Acknowledgments

Data presented in this article were provided by Wilde Engineering Sp. z o.o. company (Ltd.) in cooperation with the City Hall of Sopot.

### References

- Berberan, A., Machado, M., & Batista S. (2007). Automatic multi total station monitoring of a tunnel. *Survey Review*, 39(305), pp. 203-211. DOI: 10.1179/003962607X165177
- Bjerhammar, A. (1951). Rectangular reciprocal matrices with special reference to geodetic calculations. *Bulletin Géodésique*, pp. 188 -220
- Bond, J., Kim, D., Chrzanowski, A., & Szostak-Chrzanowski, A. (2003). Development of a fully automated, GPS based monitoring system for disaster prevention and emergency preparedness: PPMS+RT. *Sensors*, 7(7), pp. 1028-1046. DOI: 10.3390/s7071028
- Caspary, W. F. (2000). *Concepts of network and deformation analysis*. Monograph 11, School of Geomatic Engineering, The University of New South Wales, UNSW Sydney NSW 2052 Australia
- Chen, Y. Q. (1983). *Analysis of deformation surveys - A generalized method*. Technical Report No. 94, University of New Brunswick Surveying Engineering. Fredericton, N. B., Canada
- Chen, Y. Q., Chrzanowski, A. & Secord, J.M. (1990). A strategy for the analysis of the stability of reference points in deformation surveys. *CISM Journal ACSGC*, 44(2), pp. 141-149
- Chrzanowski, A., & Wilkins, R. (2006). Accuracy evaluation of geodetic monitoring of deformations in large open pit mines. *12th FIG Symposium on Deformation Measurements*, Baden, May 2006
- Daliga, K. (2014). Wpływ przezroczystej przegrody na pomiar położenia punktu tachimetrem z elektrooptycznym dalmierzem impulsowym. *Geodezja Inżynierska*. ISBN 978-83-929506-6-0, 7-26 (In Polish)
- Daliga, K., & Kuralowicz, Z. (2016). Examination method of the effect of the incidence angle of laser beam on distance measurement accuracy to surfaces with different colour and roughness. *Boletim de Ciências Geodésicas*. ISSN 1982-2170, 22(3)
- Janowski, A., Kaminski, W., Makowska, K., Szulwic, J., & Wilde, K. (2015). The method of measuring the membrane cover geometry using laser scanning and

- synchronous photogrammetry. *15th International Multidisciplinary Scientific GeoConference SGEM 2015*, www.sgem.org, SGEM2015 Conference Proceedings, ISBN 978-619-7105-34-6/ISSN 1314-2704, June 18-24 2015, Book 2 Vol. 1. DOI: 10.5593/SGEM2015/B21/S10.150
- Kohut, P., Gaska, A., Holak, K., Ostrowska, K., Sladek, J., Uhl, T., & Dworakowski, Z. (2014). A structure's deflection measurement and monitoring system supported by a vision system. *TM-Technisches Messen*, 81(12), pp. 635-643. DOI: 10.1515/teme-2014-1057
- Kowalczyk, K., & Rapinski, J. (2014). Investigating the error sources in reflectorless EDM. *Journal of Surveying Engineering*, 140(4). DOI: 10.1061/(ASCE)SU.1943-5428.0000130
- Penrose, R. (1955). A Generalized Inverse for Matrices. *Proc. Cambridge Phil. Soc.*, 51, pp. 406-413
- Perelmuter, A. (1979). Adjustment of free networks. *Bulletin Geodesique*, 53(4), pp. 291-296. DOI: 10.1007/BF02522272
- Pingue, F., Petrazzuoli, S.M., Obrizzo, F., Tammaro, U., De Martino, P., & Zuccaro, G. (2011). Monitoring system of buildings with high vulnerability in presence of slow ground deformations (The Campi Flegrei, Italy, case). *Measurement*, 44(4), pp. 1628-1644. DOI: 10.1016/j.measurement.2011.06.015
- Wilde, K., Kaminski, W., Makowska, K., Miskiewicz, M., & Szulwic, J. (2015). System of monitoring of the Forest Opera in Sopot structure and roofing. *15th International Multidisciplinary Scientific GeoConference SGEM 2015*, www.sgem.org, SGEM2015 Conference Proceedings, ISBN 978-619-7105-35-3 / ISSN 1314-2704, Book 2 Vol. 2, 471-482. DOI: 10.5593/SGEM2015/B22/S9.059
- Wiśniewski, Z. (2013). *Zaawansowane metody opracowania obserwacji geodezyjnych z przykładami*. Wyd. UWM w Olsztynie, ISBN 978-83-7299-884-2, Olsztyn, Poland (In Polish)

---

**Authors:**

MSc Daria Filipiak-Kowszyk <sup>1)</sup>, daria.filipiak@pg.gda.pl  
PhD Artur Janowski <sup>1,2)</sup>, artur.janowski@geodezja.pl  
Professor Waldemar Kamiński <sup>1,2)</sup>, waldekk@uwm.edu.pl  
MSc Karolina Makowska <sup>1)</sup>, karolina.makowska@pg.gda.pl  
PhD Jakub Szulwic <sup>1)</sup>, jakub.szulwic@geodezja.pl  
Professor Krzysztof Wilde <sup>1)</sup>, krzysztof.wilde@gmail.com

<sup>1)</sup> Gdansk University of Technology, Faculty of Civil and Environmental Engineering, Narutowicza 11-12, 80-233 Gdansk, Poland

<sup>2)</sup> University of Warmia and Mazury, Faculty of Geodesy, Geospatial and Civil Engineering, Oczapowskiego 1, 10-719 Olsztyn, Poland